

EVALUATION OF A LOAD CELL MODEL FOR DYNAMIC CALIBRATION
OF THE ROTOR SYSTEMS RESEARCH AIRCRAFT

R. W. Du Val and M. Bahrami
Advanced Rotorcraft Technology, Inc.
Los Altos, California

B. Wellman
Aeromechanics Laboratory,
U.S. Army Research & Technology Laboratories (AVSCOM)
NASA Ames Research Center
Moffett Field, California

Abstract

The Rotor Systems Research Aircraft uses load cells to isolate the rotor/transmission system from the fuselage. An analytical model of the relationship between applied rotor loads and the resulting load cell measurements is derived by applying a force-and-moment balance to the isolated rotor/transmission system. The model is then used to estimate the applied loads from measured load cell data, as obtained from a ground-based shake test. Using nominal design values for the parameters, the estimation errors, for the case of lateral forcing, were shown to be on the order of the sensor measurement noise in all but the roll axis. An unmodeled external load appears to be the source of the error in this axis.

Introduction

The Rotor Systems Research Aircraft (RSRA) has a set of seven load cells connecting the main rotor transmission to the fuselage. Their purpose is to make high-accuracy measurements of the net rotor loads, as resolved at the rotor hub, from flight data (Ref. 1). The use of these load cells to estimate applied rotor forces and moments at the hub requires an accurate mathematical expression relating rotor loads, inertial loads, and load cell readings. Both the structure and parameters of this model must be specified. Previous approaches to processing ground-test data have not yielded an acceptably accurate relationship. This is particularly true for the case of applied high frequency dynamic loads. This paper describes a new approach to obtaining the relationship, and presents the results of a preliminary evaluation of the resulting model from experimental data.

Nomenclature

| | |
|---------------------|--|
| A, B, C, D, E, F, G | - individual load cell outputs (Fig. A1) |
| a | - linear acceleration at C.G. |
| b | - position of C.G. from shaft attach point |
| d | - longitudinal distance between vertical load cell attach points |
| E{ } | - expected value operator |
| e | - lateral offset of forward lateral load cell from centerline |
| e_H | - error in estimate of applied hub loads |
| f | - lateral offset of aft lateral load cell from centerline |
| H | - vector of six applied hub loads |
| \hat{H} | - estimates of applied hub loads |
| h | - position of hub from C.G. |
| I | - moment of inertia about C.G. |
| J | - vector of six inertial loads |
| l | - position of C.G. from aft load cell attach points |
| M | - mass matrix |
| m | - effective mass of rotor/transmission/engine system |
| N_s | - number of samples |

| | |
|----------------|---|
| n | = index of measurement samples |
| p,q,r | = rotational rates about x,y,z axes |
| Q | = covariance of measurement noise |
| Q _t | = total applied engine and tail rotor drive torques |
| R | = transformation matrix for hub loads |
| S | = transformation matrix for load cells |
| T | = vector of seven load cell measurements |
| w | = lateral distance between vertical load cell attach points |
| X,Y,Z,L,M,N | = force and moment components (Fig. A2) |
| Γ | = gyroscopic coupling coefficients |
| θ | = set of unknown parameters |
| $\bar{\theta}$ | = a priori estimate of parameters |
| $\hat{\theta}$ | = post-calibration estimate of parameters |
| v | = measurement noise |
| φ,θ,ψ | = load cell deformation angles about x, y, and z axes, respectively |
| ω | = frequency |

Subscripts

| | |
|---------------|----------------------------------|
| A | = accelerometer |
| a,b,c,d,e,f,g | = attach point of each load cell |
| C | = total load |
| H | = hub load |
| I | = inertial load |
| m | = measured data |
| T | = load cell |
| x,y,z | = component for x,y,z axis |

Background

Previous Methods

The initial attempt to determine the load cell response to the applied rotor loads involved applying static loads at the hub and measuring the resulting load cell response. A least-squares regression approach was used to identify a coefficient matrix relating the seven load cells to the six hub loads. A six element bias vector was also estimated. It was found (Ref. 2) that the coefficient matrix varied as a function of the applied multiple axis load. This indicates a nonlinear dependence of the load cell response to the applied rotor loads, and would require a polynomial expansion of the multi-input multi-output relationship to characterize it in terms of constant parameters.

The next calibration was a ground-based shake test in which a pair of inertial shakers were mounted on the rotor hub to apply dynamic loads at specified amplitudes and frequencies. During this experiment, the RSRA was suspended from the hub so the static loading was the same for all tests. As a result, the nonlinear variation of the relationship with static loads observed in the static test should not be present in the shake test. The Force Determination Method (Ref. 3) was utilized to estimate applied rotor loads from a variety of sensors around the aircraft. This method first identifies the transfer functions between the applied rotor loads and sensors at various points on the aircraft, then identifies the applied rotor load from a least squares fit to the transfer functions and measured sensor responses. The results were unacceptable because the identified transfer functions varied with the magnitude of the applied load; hence, they could not be used to estimate the applied load without a more extensive calibration procedure. Since there was only one static load condition, it appears that this nonlinearity is due to a different mechanism than the nonlinearity observed in the static tests.

Proposed Method

Since the sensors utilized in the Force Determination Method (FDM) included numerous accelerometers and strain gauges mounted on the fuselage, transfer functions of these sensors will be affected by any nonlinear dynamic behavior in the fuselage. This effect complicates the use of fuselage sensors to determine applied rotor loads. The RSRA was designed to use load cells to isolate applied loads from different sources, such as the main rotor, tail rotor, engine, and wings. The

proposed approach takes advantage of this concept by treating the rotor transmission as an isolated system with externally applied loads from the load cells and the rotor (Fig. 1). The applied rotor loads are then measured from a force-and-moment balance using measured load cell loads (T) and inertial loads (J) as derived from transmission acceleration measurements. In order to utilize this approach, a model is required that relates applied external loads on the rotor/transmission system to the resulting forces and moments at the center of mass of the system. This model is derived analytically from physical principles, using the known geometry of the rotor/transmission system. Parameters with potentially uncertain values in this model are explicitly represented to provide the capability to calibrate the model.

The advantages of this approach predominantly arise from the physical insight obtained in using an analytically derived model. With such a model, sensitivity analysis and physical judgment can be used to select the most appropriate set of available parameters for calibration. Consequently, fewer parameters need be calibrated than when no physical insight is used. In addition, the parameters to be calibrated now have a physical interpretation so that the validity of the calibration results may be assessed. The model should initially be derived to be as simple as possible. If it cannot adequately explain the observed experimental behavior with a physically reasonable set of parameter values, it may be expanded to include additional effects, as required. It is important that all major effects be identified and incorporated into the model before calibration of the parameters is attempted, or the parameter values will compensate for the unmodeled effects as best they can and achieve physically unrealistic values in the process.

Objective and Approach

The objective of this study is to derive a simple dynamic model of the isolated rotor transmission system and test its accuracy with experimental data.

The approach is first to derive a simple model of the rotor transmission system, treating it as a linear, rigid, isolated body. Known or assumed values are used for all parameters of the derived model. The model is then applied to test data to determine its accuracy. If it appears that calibration can further improve the accuracy, the appropriate parameter set will be selected and calibrated. If the accuracy appears limited

by an unmodeled effect, the model will be expanded to evaluate potential sources of the unmodeled effect.

Rotor/Transmission Model

The arrangement of the load cells below the rotor/transmission system is shown in Fig. 2. A detailed description of this system, including all inertia contributions, is given in Ref. 2. There are seven load cells; four are mounted vertically at the corners of the transmission mounting plate, two are mounted laterally at the fore and aft edges of the mounting plate, and one is mounted longitudinally at the forward edge of the mounting plate. An inertial load vector, J, is located at the center of gravity of the rotor/transmission system, the applied rotor load vector (H) is located at the rotor hub (Fig. 3). The rotor hub is located at the end of the rotor shaft which is tilted forward at an angle of 2°. The load cells are connected to the transmission and the fuselage by spherical bearings.

The proposed approach is to estimate the applied hub loads from a force-and-moment balance of the external loads and the inertial loads. In order to accomplish this, all externally applied loads must be transformed to the center of mass where the inertial loads act. By treating the rotor/transmission as an isolated system, the load cell forces are considered a measured, externally applied load on the system. A 6 x 7 matrix (S) is derived that transforms the seven load cell loads (T) at their attach points to a set of six load components at the center of mass. A 6 x 6 matrix (R) is derived that transforms the applied rotor load (H) at the hub to the center of mass. An inertial load (J) at the center of mass is derived from measured accelerations and assumed inertial parameters. Using the derived matrices, a force-and-moment balance at the center of mass results in a set of six simultaneous equations which may be written in matrix form as:

$$J + S \cdot T + R \cdot H = 0 \quad (1)$$

A detailed description of these vectors and matrices are given in Appendix A.

The assumptions used in deriving the matrices and Eq. (1) are that the rotor/transmission system is a rigid body and that there is no friction in the load cell bearings. These assumptions were made to simplify the initial approach. Both nonrigid body effects and friction in the load cell bearings could be added to

the model in order to match the experimental data if that appears to be required.

The transformation matrices S and R and the inertial load vector J were all derived to explicitly contain all potentially uncertain parameters of the system, so that any subset of parameters can be selected for calibration. The parameters defined in the model are:

a) All distances and angles required to define the resultant moment arm from the center of mass to load application points.

b) All angles and magnitudes required to define load cell load components acting on the rotor/transmission system.

c) All mass properties required to determine inertial loads from measured rates and accelerations.

Test Conditions

Having derived a model, the next step is to evaluate it with experimental data. Both static and dynamic ground test data are available. The dynamic data generated by the shake test were chosen since they would provide a more rigorous test of the model structure than would the static test data. The dynamic data are not, however, suitable for testing the calibration procedure. This is because the same static load condition exists for all dynamic tests, and parameter variations are mostly dependent on variations in the static loading. Once the model structure has been validated with the dynamic data, the model can be applied to the static test data to evaluate the calibration procedure.

The test datum selected was a frequency sweep from 15 to 18.5 Hz in the y-axis applied rotor load (lateral force). This frequency range was chosen because it contains the N/rev frequency, and identification of applied rotor loads at this frequency is of special interest. The lateral forcing was chosen because previous tests have shown the poorest results with y-axis forcing, so it would provide the most rigorous test. Transfer function data were generated from the raw test data by a harmonic analyzer for four levels of applied load. Equation (1) was then used to generate the applied load estimate from the transfer function data. Equation (1) was processed with all of the model parameters set to assumed nominal values.

Error Analysis

Total Estimation Error

In a controlled ground test environment, the actual values of the applied rotor loads are known so the total error in the estimate can be readily obtained. Given the measured load cell readings, T_m , and inertial loads derived from accelerometer measurements, J_m , Eq. (1) may be used to estimate the applied rotor loads as:

$$H = -R^{-1} \cdot [J_m + S \cdot T_m] \quad (2)$$

The total error in the estimate is obtained by subtracting the known values of applied rotor load from the estimate of Eq. (2) to get:

$$e_H = H - \hat{H} = -R^{-1} \cdot [J_m + S \cdot T_m] - H \quad (3)$$

$$e_H = -R^{-1} \cdot [J_m + S \cdot T_m + R \cdot H]$$

The available shake test data were in the form of transfer functions that had been generated from the raw data by a harmonic analyzer. In order to utilize these data with the proposed model, it was necessary to transform the model to the frequency domain and write it in terms of the transfer functions. Transforming Eq. (3) to the frequency domain gives:

$$e_H(\omega) = -R^{-1} \cdot [J_m(\omega) + S \cdot T_m(\omega) + R \cdot H(\omega)] \quad (4)$$

If only a y-axis rotor load, $H_y(\omega)$, is applied, Eq. (4) may be written in terms of the transfer functions as:

$$e_H(\omega) = -R^{-1} \cdot [(J_m(\omega)/H_y(\omega)) + S \cdot (T_m(\omega)/H_y(\omega)) + R] \cdot H_y(\omega) \quad (5)$$

where $J_m(\omega)/H_y(\omega)$ and $T_m(\omega)/H_y(\omega)$ are vectors of transfer functions of the inertial and load cell loads with respect to the y-axis rotor load. Equation (5) is used to evaluate the total error in the estimate using the available transfer function data.

Numerous potential sources of error are present in this system. The evaluation procedure is to examine the total error and attempt to categorize it into the potential sources. Once identified, the sources would be modeled and included in the system. Most of the error will probably be attributable to one of five sources:

- A) Systematic errors in data collection.
- B) Unmodeled static and dynamic effects.
- C) Unmodeled external loads.
- D) Random errors in sensors.
- E) Incorrect parameter values.

Systematic Errors in Data Collection

One source of error is the use of transfer function data. Since this is treated as raw data in this study, any errors in the identification of the transfer functions would propagate through the proposed approach. The recorded time domain data should be reprocessed by the harmonic analyzer to provide only Fourier transformed data, not transfer functions.

Angular accelerometers and rate gyros were not available on the rotor transmission system for the shake test. Since there is no way to obtain all such data, the approach taken is to assume it is negligible and see how the estimates compare with this assumption. Some justification for this assumption comes from comparing the response of the two linear accelerometers mounted on the transmission with a 2-ft vertical displacement between them. The difference in the y-axis components divided by the vertical displacement should give the roll axis angular acceleration. The average value of this derived roll acceleration over the frequency range for an applied load of 800 lb was found to be 0.09 rad/sec/sec, supporting the low angular acceleration assumption. The derived angular acceleration data was not used with the model because the errors in the linear accelerometers are such that the accuracy of the derived angular acceleration is 0.6 rad/sec/sec. The derived values are therefore in the noise level. The angular acceleration affects the translational equations since the linear accelerometer is not mounted at the center of mass and will, therefore, be affected by angular accelerations. The moment equations are affected since the angular inertial loads are dependent on the angular accelerations. The errors associated with neglecting a

0.09 rad/sec/sec roll angular acceleration are 12 lb in the y-force and 27 ft-lb in the rolling moment so the assumption appears justified.

Unmodeled Static and Dynamic Effects

The model derived for this study was kept deliberately simple to facilitate the analysis. It can be expanded if necessary to account for the observed error. Unmodeled effects with potentially significant impact on the model include friction in the load cell bearings, flexibility in the rotor/transmission system and nonlinearity in the dynamic response to applied loads. The nature of the error signal should suggest which of these effects are present. Friction and deadbands will be characterized by hysteresis in the response. This effect is more readily observed in static data than in dynamic data. Flexibility will show up as a resonance at some frequency and will result in a phase and amplitude shift between the input and output signals. Nonlinear dynamics will be readily detected by a frequency shift between the input and output data. Static nonlinearities result in parameter variations and are corrected by calibration rather than by expanding the model.

Random Errors in Sensors

Both load cells and accelerometers have measurement noise that produces a lower bound on the accuracy of the applied load estimates. It is possible to obtain accuracies below this limit, but this requires the use of statistical processing techniques such as Kalman Filtering and Smoothing. This effect can certainly not be reduced by any modifications to the model. The effect of accelerometer and load cell noise on the applied rotor load estimate is derived in Appendix B and used to generate the errors given in Table I. These numbers were based on the assumption of independent random errors for each sensor with accuracies of 1% of full scale for the accelerometers and 0.1% of full scale for the load cells.

Unmodeled External Loads

The derived model will be in error if all externally applied loads are not included. If the levels are low, then this can be the most difficult source of error to identify. This is because it can take on virtually any characteristic and will blend in with other error sources. The only possibility for detecting this type of error is if it is sufficiently large that it cannot be logically explained by any of the other error

sources. Once the presence of an unmodeled load is suspected, the error data may assist in isolating its source, but a thorough examination of the test conditions is usually required to resolve this effect.

Incorrect Parameter Values

once the model structure has been validated to the fullest extent possible, the remaining errors should be due only to incorrect values for the parameters. At this point, calibration may be applied to reduce this error source. If calibration is attempted before the model structure is adequately determined, the parameters will take on whatever values are required to compensate for the model structure errors. This will result in physically unrealistic values for the parameters and could, in fact, be a test for whether the model structure is accurate.

The conventional approach to calibration has been to apply least-squares minimization of the error with respect to the parameters to be calibrated. Since the parameters are now imbedded in a model, the least-squares minimization of the error must be done subject to the constraint that the model equations are satisfied. This is referred to as a constrained least-squares approach (Ref. 4) and the algorithm is derived in Appendix C for the constraint of Eq. (1).

Since the available data are in the frequency domain, the calibration must be performed in the frequency domain. This is actually an advantage since the frequency domain transformation has concentrated information for the required frequency range into fewer data points than required for a time domain representation. Calibration may then be performed with fewer data in the frequency domain. The least-squares minimization may be applied to frequency domain data in the same way as it is applied to time domain data (Ref. 5). The only modification is that the data are organized with the real and imaginary parts stacked end to end rather than using the data in complex form. This insures that the identified parameter values will not be complex.

Results

Equation (3) was applied to transfer function data for the load cells and the main rotor gear box accelerometers to generate the estimation error of the derived model in the frequency domain. Assumed, nominal values, based on aircraft design specifications, were used for all parameters in the model. Figures 4 and 5

show the magnitude of the transfer function data for the seven load cells and two accelerometers for an 800 lb y-axis excitation. The location of the load cells may be seen by finding the correspondingly labeled load cell in Fig. 2. The accelerometer transfer functions have been multiplied by the system mass to produce inertial loads. The strong coupling in the system is apparent from the large vertical load cell values for a y-axis excitation. The strong correlation in the z-axis is particularly apparent from the sudden drop in z-axis acceleration at the same frequency (16.6 Hz) where two vertical load cells (A and B) suddenly assume equal and opposite values.

Figures 6 through 11 show the error in the model, as defined by Eq. (3), using nominal parameter values. Table I shows the average error over the frequency range as compared to the accuracy limit set by the instrumentation noise. With the exception of applied rolling moment, the average error shown in Table I and the frequency plots shown in Figs. 6-11 demonstrate that the rigid body model of the isolated rotor transmission system produces applied load estimates with error levels comparable to the instrumentation noise level.

The pronounced roll moment error (Fig. 9) is too great to be explained by parameter errors, sensor errors, or angular accelerations. The demonstrated lack of significant angular accelerations about the roll axis indicates that it is not due to a nonrigid body effect. It can also be seen that there is no frequency shift (the hump at 16.6 Hz in the error signal matches the hump in the load cell data at that frequency) so the error is not a nonlinear function of the modeled variables. The only remaining explanation is that the error is due to an unmodeled external load with predominant effect in the roll axis. A potential candidate for the source of this load is the drive train since it would affect only the roll moment. Measurements of the shaft torques from the engine and the tail rotor are required to verify this and could be used to compensate for this effect.

Nominal parameter values produce estimation errors on the order of the instrumentation noise level in all but the roll axis, and the roll axis error is too great to be explained by parameter uncertainties; therefore, calibration is not needed to improve the accuracy in five axes and would not help in the sixth. The source of unknown roll axis loading must be determined and modeled before the model can be used for roll moment estimation.

Conclusions

An analytically derived model with nominal parameter values has been used to estimate applied rotor loads from measured load cell and accelerometer data. This approach has also provided a check on the consistency of measured input/output data. The presence of an unmodeled external load was detected in the roll axis and its source is being investigated.

The following conclusions are drawn from this work:

For the y-axis case, an analytically derived linear, rigid body model of the isolated rotor/transmission system with nominal parameter values performs well in all but the roll axis.

Nonrigid body effects or nonlinear behavior cannot explain the roll moment error. The error must be due to an externally applied, unmodeled load.

Calibration is unnecessary for this case since improved parameter estimates will not improve the estimation error further. The estimation error in all but the roll axis is already in the noise level and the error in the roll axis is too great to be logically explained by different parameter values.

Recommendations for Further Research

The following recommendations are made:

Apply the model to data generated by excitation in other axes to validate it under a broader range of conditions and to further isolate the source of the unmodeled load. This analysis should be backed up by a follow-on physical error source analysis.

Apply the model to static test data to evaluate the calibration technique. Nominal parameter values have done surprisingly well in allowing accurate hub load estimation for the specific static load condition present in the dynamic data. Static test experience suggests that this will not be true under all static load conditions. Once the model structure is fully validated it should be applied to static test data to determine which parameters to calibrate and to determine the range of variation of the parameters through calibration.

Appendix A: Load Cell Model Derivation

A diagram of the undeformed load cell geometry is shown in Fig. A1. The load cells are mounted to the fuselage and to the transmission base by spherical bearings. It is assumed that the transmission base does not warp, so all changes in the load cell geometry are due to deformations in the load cells themselves or in the fuselage mounting points. With this assumption it is possible to completely model the load cell response using a general three-component representation of the reaction force at each attach point on the transmission base; no knowledge of the fuselage deformation is required.

Three plane views of the load cell geometry with the three-component reaction force representation are shown in Fig. A2. Inertial loads, including gravity and the drive shaft torque, are assumed to be concentrated at the transmission center of gravity. The rotor loads are concentrated at the hub. Taking the sum of the forces and moments about the center of gravity gives:

$$X_C = X_I + X_H + G_x + E_x + F_x + A_x \\ + B_x + C_x + D_x = 0$$

$$Y_C = Y_I + Y_H + G_y + E_y + F_y + A_y \\ + B_y + C_y + D_y = 0$$

$$Z_C = Z_I + Z_H + G_z + E_z + F_z + A_z \\ + B_z + C_z + D_z = 0$$

$$L_C = L_I + L_H + Y_H \cdot h_z + (A_z + D_z) \cdot w/2 \\ E_z \cdot e - (B_z + C_z) \cdot w/2 + F_z \cdot f \\ - (B_y + C_y + F_y + G_y + E_y + A_y + D_y) \\ \cdot b_z = 0$$

$$M_C = M_I + M_H - X_H \cdot h_z - Z_H \cdot h_x \\ - (B_z + A_z + E_z + G_z) \cdot (d - 1) \\ + (C_x + D_x + F_x + B_x + A_x + E_x + G_x) \\ \cdot b_z + (C_z + D_z + F_z) \cdot 1 = 0$$

$$\begin{aligned}
N_C = & N_I + N_H + (A_y + E_y + G_y + B_y) \\
& \cdot (d - 1) - (C_y + F_y + D_y) \cdot 1 \\
& - (A_x + D_x) \cdot w/2 - E_x \cdot e + (C_x \\
& + B_x) \cdot w/2 - F_x \cdot f + Y_H \cdot h_x = 0
\end{aligned}
\tag{A1}$$

Using the transformations:

$$\begin{aligned}
A_x &= A \cos(\phi_a) \sin(\theta_a) \\
A_y &= -A \sin(\phi_a) \\
A_z &= A \cos(\phi_a) \cos(\theta_a) \\
B_x &= B \cos(\phi_b) \sin(\theta_b) \\
B_y &= -B \sin(\phi_b) \\
B_z &= B \cos(\phi_b) \cos(\theta_b) \\
C_x &= C \cos(\phi_c) \sin(\theta_c) \\
C_y &= -C \sin(\phi_c) \\
C_z &= C \cos(\phi_c) \cos(\theta_c) \\
D_x &= D \cos(\phi_d) \sin(\theta_d) \\
D_y &= -D \sin(\phi_d) \\
D_z &= D \cos(\phi_d) \cos(\theta_d) \\
E_x &= -E \cos(\phi_e) \sin(\psi_e) \\
E_y &= E \cos(\phi_e) \cos(\psi_e) \\
E_z &= E \sin(\phi_e) \\
F_x &= F \cos(\phi_f) \sin(\psi_f) \\
F_y &= -F \cos(\phi_f) \cos(\psi_f) \\
F_z &= -F \sin(\phi_f) \\
G_x &= G \cos(\theta_g) \cos(\psi_g) \\
G_y &= G \cos(\theta_g) \sin(\psi_g) \\
G_z &= -G \sin(\theta_g)
\end{aligned}
\tag{A2}$$

the equations become

$$J + R \cdot H + L \cdot T = 0 \tag{A3}$$

where:

$$J' = [X_I, Y_I, Z_I, L_I, M_I, N_I] \tag{A4}$$

and

$$\begin{bmatrix} X_I \\ Y_I \\ Z_I \\ L_I \\ M_I \\ N_I \end{bmatrix} = \begin{bmatrix} -m_x \cdot a_x \\ -m_y \cdot a_y + \Gamma_y \cdot q \\ -m_z \cdot a_z \\ -I_x \cdot p + Qt + \Gamma_L \cdot q \\ -I_y \cdot q + \Gamma_M \cdot p \\ -I_z \cdot r \end{bmatrix} \tag{A5}$$

In Eq. (A5), a_x , a_y , and a_z are linear accelerations in each direction measured at the rotor/transmission system center of gravity, and p , q , and r are rotational accelerations. Because of the nonrigid engine mountings, the engine contributions to inertial forces are not equal in all directions when measured at the system center of gravity. This effect can be adequately modeled by assigning different values to the total effective mass of the combined rotor/transmission/engine system in each direction: m_x , m_y , and m_z . There are also a few minor error terms not given here that are discussed fully in Ref. 2. I_x , I_y , and I_z are moments of inertia; related terms in the cross-products of rotational rates are negligible. Qt is total applied engine and tail rotor shaft torque. Gyroscopic coupling forces due to engine and transmission rotational moments of momentum are represented by the coefficients Γ , with subscripts for the appropriate axis. The hub forces (H) and load cell readings (T) in Eq. (A3) are given by:

$$H' = [X_H, Y_H, Z_H, L_H, M_H, N_H] \tag{A6}$$

$$T' = [A, B, C, D, E, F, G] \tag{A7}$$

The geometric transformations from the applied loads to the center of mass (R and S) are given by:

$$R = \begin{bmatrix} 1 & 0 & 0 & 0 & 0 & 0 \\ 0 & 1 & 0 & 0 & 0 & 0 \\ 0 & 0 & 1 & 0 & 0 & 0 \\ 0 & h_z & 0 & 1 & 0 & 0 \\ -h_z & 0 & -h_x & 0 & 1 & 0 \\ 0 & h_x & 0 & 0 & 0 & 1 \end{bmatrix} \tag{A8}$$

ORIGINAL PAGE IS
OF POOR QUALITY

and

$$S = \begin{bmatrix} C\phi aS\theta a & C\phi bS\theta b & C\phi cS\theta c & C\phi dS\theta d & -C\phi eS\psi e & -C\phi fS\psi f & C\phi gC\psi g \\ -S\phi a & -S\phi b & -S\phi c & -S\phi d & C\phi eC\psi e & C\phi fC\psi f & C\phi gS\psi g \\ C\phi aC\theta a & C\phi bC\theta b & C\phi cC\theta c & C\phi dC\theta d & S\phi e & S\phi f & -S\theta g \\ w/2C\phi aC\theta a & bzS\phi b & bzS\phi c & bzS\phi d & -eS\phi e & -fS\phi f & -bzC\phi gS\psi g \\ +bzS\phi a & -w/2C\phi bc\theta b & -w/2C\phi cc\theta c & +w/2C\phi dd\theta d & -bzC\phi eC\psi e & +bzC\phi fC\psi f & \\ bzC\phi aS\theta a & bzC\phi bS\theta b & bzC\phi cS\theta c & bzC\phi dS\theta d & -bzC\phi eS\psi e & +bzC\phi fS\psi f & bzC\theta gC\psi g \\ -(d-1)C\phi aC\theta a & -(d-1)C\phi bC\theta b & +1C\phi cC\theta c & +1C\phi dC\theta d & -(d-1)S\phi e & +1S\phi f & +(d-1)S\theta g \\ -w/2C\phi aC\theta a & w/2C\phi bS\theta b & 1S\phi c & 1S\phi d & -eC\phi eS\psi e & +1C\phi fC\psi f & (d-1)C\theta gS\psi g \\ -(d-1)S\phi a & -(d-1)S\phi b & +w/2C\phi cc\theta c & -w/2C\phi dd\theta d & +(d-1)C\phi eC\psi e & -fC\phi fS\psi f & \end{bmatrix} \quad (A9)$$

where C and S denote cosine and sine functions, respectively

Appendix B: The Effect of Sensor Noise on Load Estimation

The analytical model of the rotor/transmission system derived in the text has the form:

$$J + S \cdot T + R \cdot H = 0 \quad (B1)$$

Given the measured load cell readings, T_m , and inertial loads derived from accelerometer measurements, J_m , the applied rotor loads, H , are estimated from Eq. (B1) as:

$$H = -R^{-1} \cdot [J_m + S \cdot T_m] \quad (B2)$$

The measured load cell and accelerometer values may be written in terms of their true values and a random measurement noise component as follows.

$$a_m = a + v_A, \quad v_A = N(0, Q_A) \quad (B3)$$

$$T_m = T + v_T, \quad v_T = N(0, Q_T) \quad (B4)$$

Writing the derived inertial load vector, J_m , as the product of an inertia matrix, M , and the accelerometer measurements, a_m , gives

$$J_m = M \cdot a_m = M \cdot a + M \cdot v_A = J + M \cdot v_A \quad (B5)$$

where J is the actual inertial load vector.

Substituting Eqs. (B4) and (B5) into Eq. (B2) gives:

$$H = -R^{-1} \cdot [J + S \cdot T] + v_H \quad (B6)$$

where

$$v_H = -R^{-1} \cdot [M \cdot v_A + S \cdot v_T] \quad (B7)$$

Substituting Eq. (B1) into Eq. (B6) then gives:

$$H = H + v_H, \quad v_H = N(0, Q_H) \quad (B8)$$

From Eq. (B8) it is seen that v_H , as given by Eq. (B7), is the combined effect of the instrumentation errors on the applied rotor load estimate, H . This error represents a lower bound on the accuracy of the estimation that is attainable without applying statistical processing, such as Kalman filtering or smoothing. The covariance of this error, Q_H , may be computed from Eq. (B7) using the known covariance of the instrumentation errors, Q_A and Q_T , as follows.

$$\begin{aligned} Q_H &= E\{v_H v_H^T\} \\ &= E\{[-R^{-1} \cdot (M \cdot v_A + S \cdot v_T)] \\ &\quad \cdot [-R^{-1} \cdot (M \cdot v_A + S \cdot v_T)]^T\} \end{aligned} \quad (B9)$$

$$\begin{aligned} Q_H &= R^{-1} \cdot M \cdot E\{v_A v_A^T\} \cdot M^T \cdot (R^{-1})^T \\ &\quad + S \cdot E\{v_T v_T^T\} \cdot S^T \cdot (R^{-1})^T \\ &\quad + R^{-1} \cdot M \cdot E\{v_A v_T^T\} \cdot M^T \cdot (R^{-1})^T \\ &\quad + S \cdot E\{v_T v_A^T\} \cdot M^T \cdot (R^{-1})^T \\ &\quad + R^{-1} \cdot M \cdot E\{v_A v_T^T\} \cdot S^T \cdot (R^{-1})^T \\ &\quad + R^{-1} \cdot S \cdot E\{v_T v_T^T\} \cdot S^T \cdot (R^{-1})^T \end{aligned}$$

(B10)

The sensor noise components are assumed independent so the term $E\{v_A v_A^T\}$ is zero. Substituting the known covariance matrices of the sensors for the other expected value terms gives:

$$Q_H = R^{-1} \cdot [M \quad Q_A \cdot M' + S \cdot Q_T \cdot S'] \cdot (R^{-1})' \quad (B11)$$

Appendix C: Calibration Algorithm

The applied rotor load estimation error is given by Eq. (3) in the text as:

$$e_H = \hat{\theta} - \theta = [J_m + S \cdot T_m + R \cdot H]^{-1} \cdot e_H \quad (C1)$$

The coefficient matrices, R and S contain geometric parameters of the model and the derived inertial loads vector, include inertial parameters of the model. A subset, θ , of the parameters is selected for calibration and the error is treated as a function of those parameters. A cost function is written in the form:

$$V(\theta) = 1/2 \cdot \sum_{n=1}^{N_s} e_H(\theta, n)' \cdot W^{-1} \cdot e_H(\theta, n) \quad (C2)$$

where W is a weighting matrix given by:

$$W = 1/N_s \cdot \sum_{n=1}^{N_s} e_H(\theta, n) \cdot e_H(\theta, n)' \quad (C3)$$

Expanding the first partial of V with respect to the parameter set θ about their nominal values of $\bar{\theta}$ gives:

$$\partial V(\hat{\theta})/\partial \theta = \partial V(\bar{\theta})/\partial \theta + (\hat{\theta} - \bar{\theta}) \cdot \partial^2 V(\bar{\theta})/\partial \theta^2 \quad (C4)$$

Setting the desired value at $\hat{\theta}$ to zero, corresponding to an extremum, gives:

$$\hat{\theta} = \bar{\theta} - (\partial^2 V(\bar{\theta})/\partial \theta^2)^{-1} \cdot (\partial V(\bar{\theta})/\partial \theta)' \quad (C5)$$

Taking the first partial of V with respect to θ gives:

$$\partial V(\bar{\theta})/\partial \theta = \sum_{n=1}^{N_s} e_H(\bar{\theta}, n)' \cdot W^{-1} \cdot \partial e_H(\bar{\theta}, n)/\partial \theta \quad (C6)$$

The second partial, to first order, is then:

$$\partial^2 V(\bar{\theta})/\partial \theta^2 = \sum_{n=1}^{N_s} (\partial e_H(\bar{\theta}, n)/\partial \theta)' \cdot W^{-1} \cdot \partial e_H(\bar{\theta}, n)/\partial \theta \quad (C7)$$

Once the parameter set has been chosen, the partial derivative of the errors, e_H , with respect to the parameters must be generated analytically from Eq. (C1). The parameter estimates are then obtained from Eqs. (C5) to (C7) using the measurement error sequence, e_H , generated by Eq. (C1).

References

1. Burks, J. S., "Rotor Systems Research Aircraft (RSRA) Rotor Force and Moment Measurement System," AIAA First Flight Test Conference, Las Vegas, Nev., Nov. 1981.
2. Acree, C. W., "Results of the First Complete Static Calibration of the RSRA Rotor Load Measurement System," NASA TP-2327, 1984.
3. Giansante, N., Berman, A., Flannely, W. G., and Nagy, E. J., "Structural System Identification Technology Verification," USAAVRADCOR Report No. TR-81-D-28, Nov. 1981.
4. Bryson, A. E., Jr., and Ho, Y. C., Applied Optimal Control, Blaisdell Publishing Co., Waltham, Mass., 1969.
5. Du Val, R. W., "The Use of Frequency Methods in Rotorcraft System Identification," AIAA Paper 81-2386, AIAA 1st Flight Testing Conference, Las Vegas, Nev., Nov. 1981.

C-5

ORIGINAL PAGE IS
OF POOR QUALITY

Table I

| Load | Estimation error | | | | Instrumentation noise | | |
|------|------------------|--------|--------|--------|-----------------------|------------|----------------|
| | 200 lb | 400 lb | 600 lb | 800 lb | Total | Load cells | Accelerometers |
| X | 84 | 76 | 173 | 214 | 309 | 25 | 308 |
| Y | 10 | 25 | 35 | 96 | 312 | 35 | 308 |
| Z | 12 | 17 | 28 | 39 | 312 | 50 | 308 |
| L | 592 | 1648 | 1772 | 2477 | 446 | 179 | 408 |
| M | 27 | 17 | 24 | 47 | 436 | 143 | 412 |
| N | 84 | 76 | 173 | 214 | 81 | 61 | 54 |

Load cell full scale = 25,000 lb, error = 0.1%
Accelerometer full scale = 7 G's, error = 1%
Mass = 4400 lb

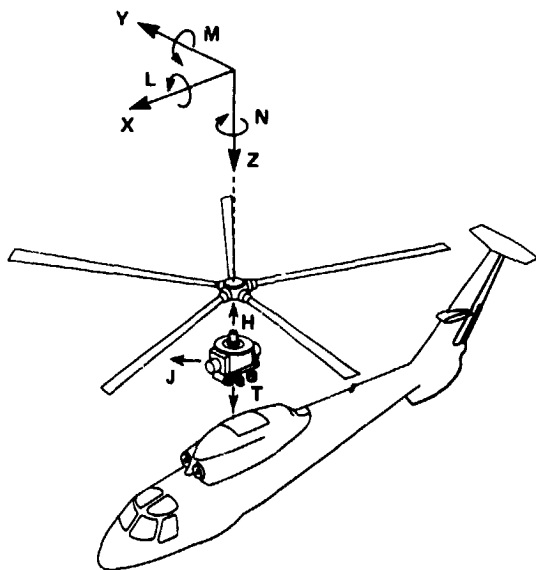


Fig. 1 Loads acting on isolated rotor/transmission system.

MAIN ROTOR LOAD MEASUREMENT SYSTEM

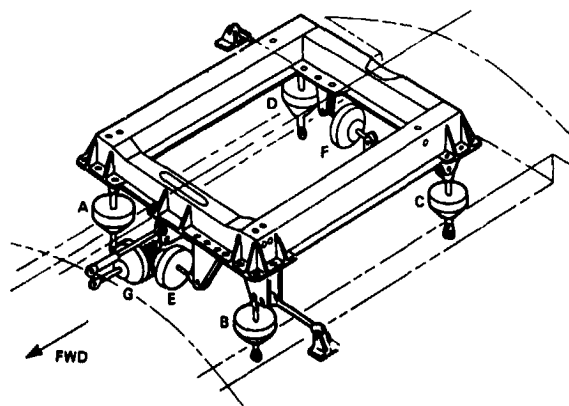


Fig. 2 Load cell arrangement for rotor/transmission system.

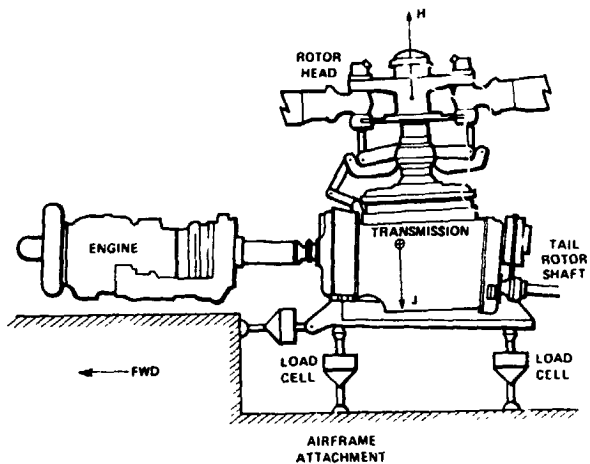


Fig. 3 Rotor/transmission system.

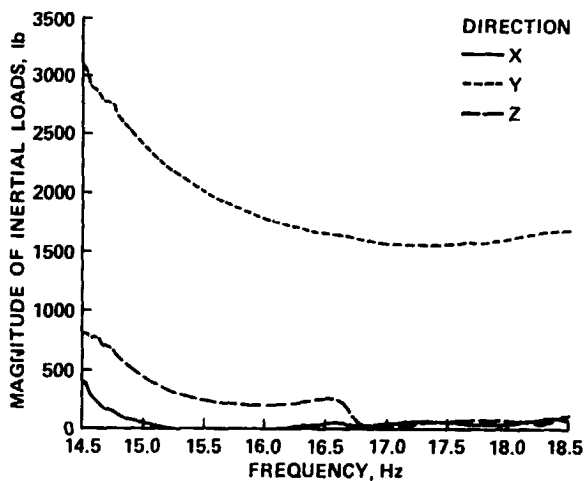


Fig. 5 Magnitude of inertial load transfer functions for 800 lb. applied lateral force.

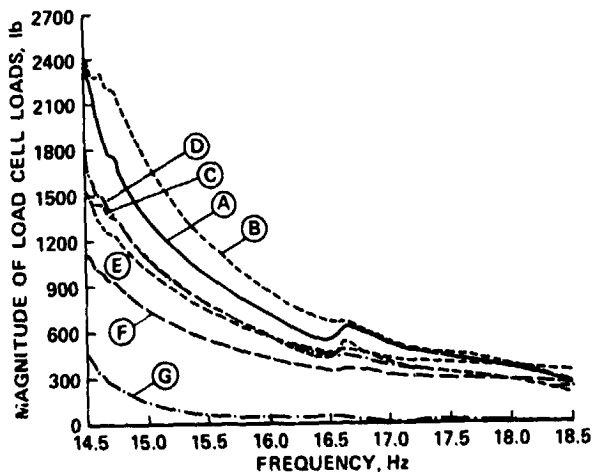


Fig. 4 Magnitude of load cell transfer functions for 800 lb. applied lateral force.

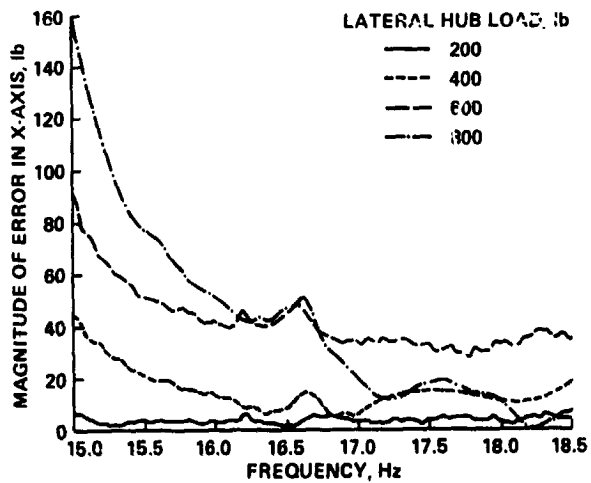


Fig. 6 Magnitude of x-axis applied force estimation error.

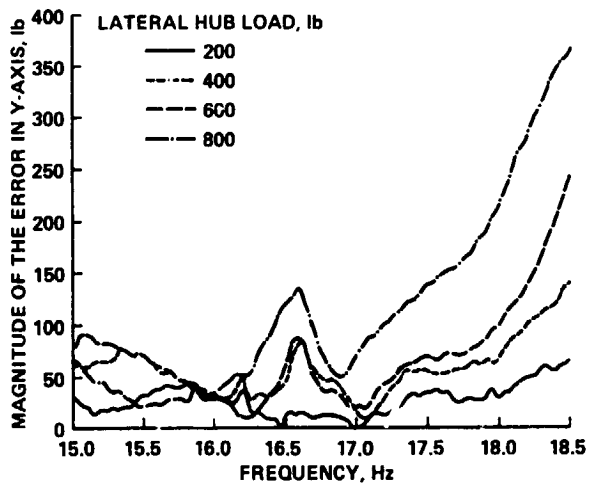


Fig. 7 Magnitude of y-axis applied force estimation error.

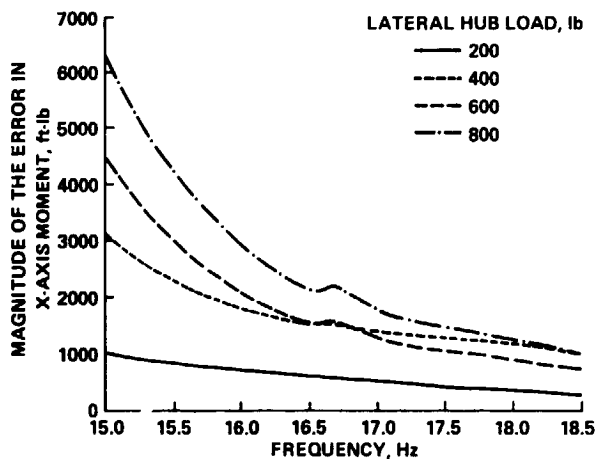


Fig. 9 Magnitude of x-axis applied moment estimation error.

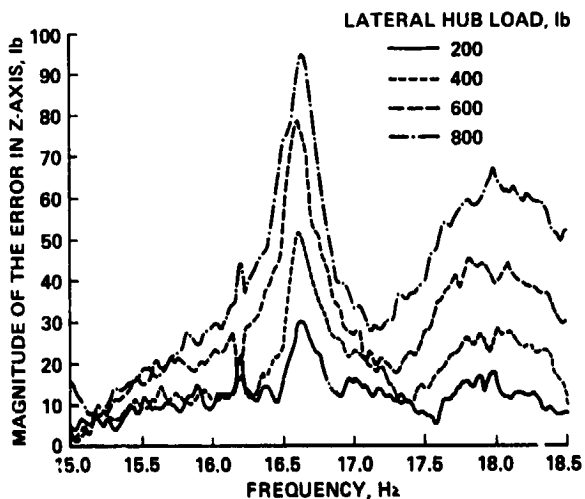


Fig. 8 Magnitude of z-axis applied force estimation error.

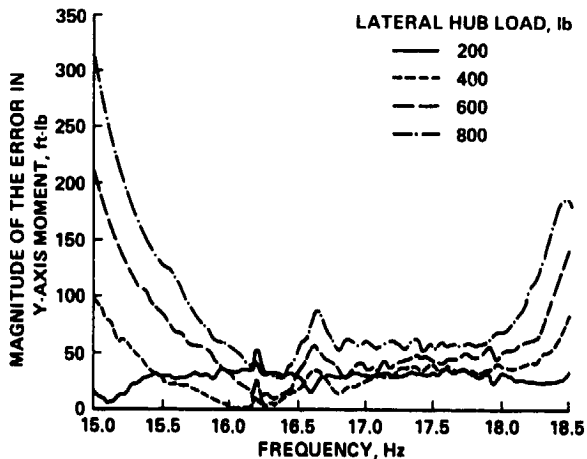


Fig. 10 Magnitude of y-axis applied moment estimation error.

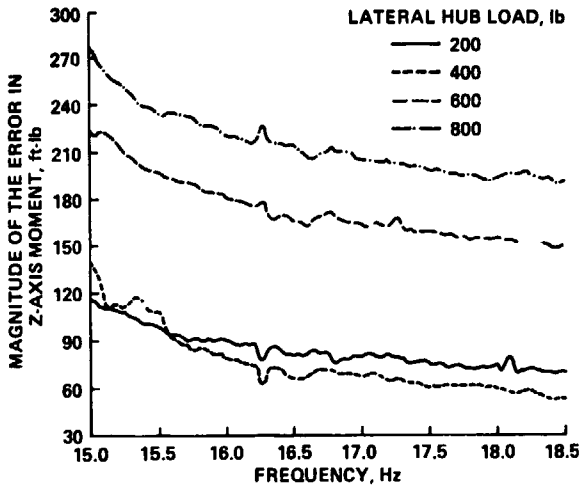


Fig. 11 Magnitude of z-axis applied moment estimation error.

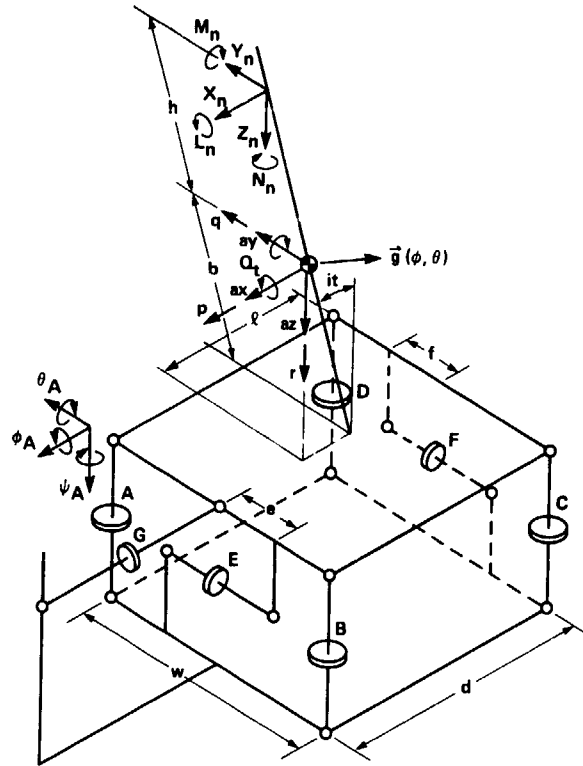
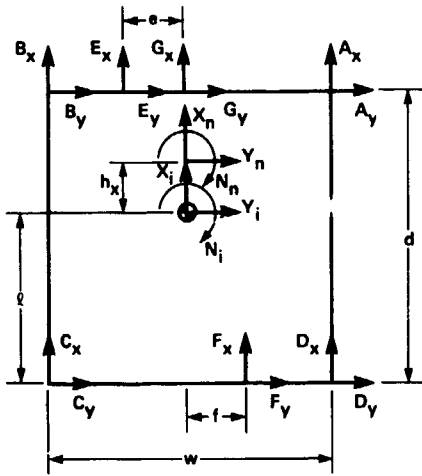
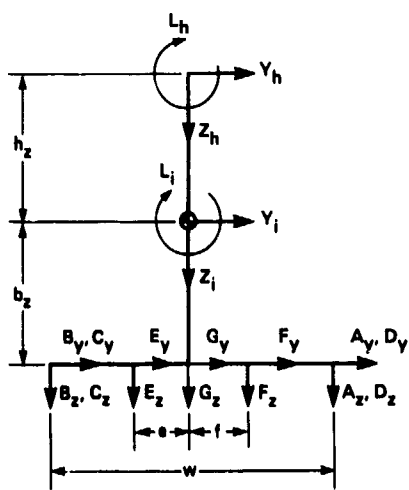


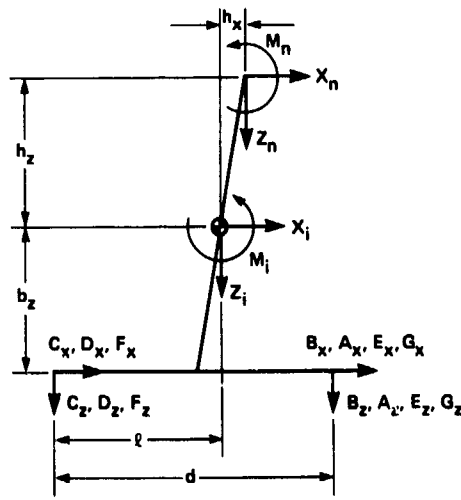
Fig. A1 Undeformed load cell geometry.



TOP VIEW



REAR VIEW



SIDE VIEW

Fig. A2 Load cell geometry with generalized reaction force components.

DISCUSSION
Paper No. 24

EVALUATION OF A LOAD CELL MODEL FOR DYNAMIC CALIBRATION OF THE ROTOR SYSTEM RESEARCH AIRCRAFT

R. W. Du Val
M. Bahrami
and
B. Wellman

Charlie Fredrickson, Sikorsky Aircraft: I'd like to thank you for your paper and for mentioning the drive train and its possible impact on rotor loading, transmission loading, etc. One effect that you may not have modeled seems to be kind of glaring and looking at the analytical model in your paper was the engine. I see the engine kind of cantilevered off the transmission [or] the drive shaft and I am sure that is not the way it is supported. If it does have a longitudinal restraint to the airframe that may account for part of the modeling error that you may not have accounted for.

Du Val: Yes, in fact the way the engine is mounted is that there are swivel mounts in a universal joint that should prevent any longitudinal restraint on the engine. Now just how well those are working is another question.

Dev Banerjee, Hughes Helicopters: Ron, a very logical and systematic modeling approach to identifying the model of the transmission mount. When you get to correlating the test results with your analytical model, I presume you would include the noise characteristics into your error function. How do you intend putting in the covariance of the noise of the load cell? [How do you] intend to find it?

Du Val: That basically was done analytically. Since we have a covariance for the load cells and for the accelerometers we can use our analytical model to determine what the resulting covariance would be in the estimation of the hub loads, using those assumed covariances for the sensor data, and in fact that is the way we arrived at the noise level lines that we put on the charts.